COSMIC BACKGROUND EXPLORER (COBE) OBSERVATIONS: NEW SKY MAPS OF THE EARLY UNIVERSE

GEORGE. F. SMOOT
Lawrence Berkeley Laboratory and Space Sciences Laboratory,
Bldg 50-352 - 1 Cyclotron Road
University of California, Berkeley, 94720

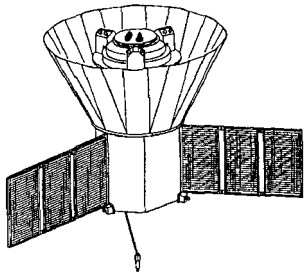

ABSTRACT

This paper presents early results obtained from the first six months of measurements of the Cosmic Microwave Background (CMB) by instruments aboard NASA's Cosmic Background Explorer (*COBE*)* satellite and discusses the implications for cosmology. The three instruments: FIRAS, DMR, and DIRBE have operated well and produced significant new results. The FIRAS measurement of the CMB spectrum supports the standard Big Bang model. The maps made from the DMR instrument measurements show a spatially smooth early universe. The measurements are sufficiently precise that we must pay careful attention to potential systematic errors. The maps of galactic and local emission produced by the DIRBE instrument will be needed to identify foregrounds from extragalactic emission and thus to interpret the results in terms of events in the early universe.

* The National Aeronautics and Space Administration/Goddard Space Flight Center is responsible for the design, development, and operation of the Cosmic Background Explorer. GSFC is also responsible for the software development through to the final processing of the space data. The *COBE* program is supported by the Astrophysics division of NASA's Office of Space Science and Applications.

1. INTRODUCTION

The standard cosmological model was established in 1965 with the discovery of the cosmic microwave background (CMB) and the recognition of its implications. In the (Friedmann-Robertson-Walker) Big Bang model cosmologists had a theoretical framework for describing the development of the universe from a time of about one hundredth of a second through the present age of the universe. The most notable and precise successes of the Big Bang model were the calculation of the primordial nucleosynthesis of the light elements (notably ^{4}He, ^{3}He, D, T, and ^{7}Li) and the existence of a thermal relic radiation (CMB) from this era."The First Three Minutes" by Steve Weinberg (1977) and "Physical Cosmology" by Jim Peebles (1971) provide an excellent account of this model.

With the development of the Standard Model of strong and electroweak interactions providing a theory of physics up to the weak scale (250 GeV) and ideas about grand unification, particle theory has provided a context and motivation for extending and expanding the original Big Bang model. That fundamental particles (quarks and leptons) are point like particles with asymptotic freedom from strong interactions at high energies provides a picture of the early universe as a dilute gas of weakly interacting quarks, leptons, and guage bosons. This picture is more readily understandable than the old view of the hadron era (10^{-5} sec), when many particles were crowded together with separations and horizons less than a typical particle size (e.g. a proton). With this context it has been possible to develop a senario of the universe from very early times (10^{-35} sec) including a phase transition induced period of inflation, a time of baryogenesis, and other events leading to the original Big Bang model including the fluctuations that lead to galaxy and other structure formation. In this standard model cosmology and particle physics come together for inspiration and consistency and the observations and experiments in each constrain and test each others models. "The Early Universe" by Rocky Kolb and Mike Turner is my recommended description of this extended standard model.

The light elements and the cosmic microwave background (CMB) are the most accessible relics from the eras during which the universe was a relatively structureless plasma prior to its evolving to the highly-ordered state observed today. In standard models of cosmology, CMB photons have travelled unhindered from the surface of last scattering in the early universe to the present era; as such, the CMB maps the large scale structure of space-time in the early universe. Despite a quarter-century of effort, no intrinsic anisotropy in the CMB has been detected. Likewise, there has been a fruitless search for distortions of the spectrum from a featureless blackbody. These measurements can constrain possible effects in the early universe and cosmology and particle physics theories.

The *COBE* (Cosmic Background Explorer satellite) experiments were designed and have turned out to be a precision test of the standard model of cosmology. *COBE* was launched on November 18, 1989 into a 900-km circular, near-polar orbit (inclination 99°). The Earth's gravitational quadrupole moment precesses the orbit to follow the terminator, allowing the instruments to point away from the Earth and perpendicular to the Sun to avoid both solar and terrestrial radiation. Throughout most of the year, the satellite orbit provides an exceptionally stable environment. During the two months surrounding summer solstice, the satellite is unable to shield the instruments and dewar from the Earth and Sun simultaneously, and the Earth limb becomes visible over the shielding surrounding the instrument aperture plane as the satellite passes over the North Pole. During the same period, the satellite enters the Earth's shadow as the orbit crosses over the South Pole. Prior to depletion of the liquid helium cryogen on September 20, 1990, the DIRBE and FIRAS instruments mapped the sky 1.6 times. As the dewar warms, the DIRBE instrument continues to take data in its four shortest wavelength bands. The DMR instrument does not require cryogenic cooling and continues to operate normally.

The *COBE* Science Working Group (SWG), consisting of C. L. Bennett, N. W. Boggess, E. S. Cheng, E. Dwek, S. Gulkis, M. G. Hauser, M. Janssen, T. Kelsall, P. Lubin, J. C. Mather, S. Meyer, S. H. Moseley, T. L. Murdock, R. A. Shafer, R. F. Silverberg, G. F. Smoot, R. Weiss, D. T. Wilkinson, and E. L.Wright, is responsible for the scientific oversight.

2. The DIRBE Instrument Description and Preliminary Results

The Diffuse Infrared Background Experiment (DIRBE) is designed to conduct a sensitive search for an isotropic cosmic infrared background (CIB) radiation over the spectral range from 1 to 300 microns. The cumulative emissions of pregalactic, protogalactic, and evolving galactic systems are expected to be recorded in this background. Since both the cosmic red-shift and reprocessing of short-wavelength radiation to longer wavelengths by dust act to shift the short-wavelength emissions of cosmic sources toward or into the infrared, the spectral range from 1 to 1000 microns is expected to contain much of the energy released since the formation of luminous objects, and could potentially contain a total radiant energy density comparable to that of the CMB. The discovery and measurement of the CIB would provide new insight into the cosmic 'dark ages' following the decoupling of matter and the CMB.

Observing the CIB is a formidable task. Bright foregrounds from the atmosphere of the Earth, from interplanetary dust scattering of sunlight and emission of absorbed sunlight, and from stellar and interstellar emissions of our own Galaxy dominate the diffuse sky brightness in the infrared. Even when measurements are made from space with cryogenically-cooled instruments, the local astrophysical foregrounds strongly constrain our ability to measure and discriminate an extragalactic infrared background. Furthermore, since the absolute brightness of the CIB is of paramount interest for cosmology, such measurements must be done relative to a well-established absolute flux reference, with instruments which strongly exclude or permit discrimination of all stray sources of radiation or offset signals which could mimic a cosmic signal.

The DIRBE approach is to obtain absolute brightness maps of the full sky in 10 photometric bands (J[1.2], K[2.3], L[3.4], and M[4.9]; the four *IRAS* bands at 12, 25, 60, and 100 micrometers; and 120-200 and 200-300 micrometer bands). To facilitate determination of the bright foreground contribution from interplanetary dust, linear polarization is also measured in the J, K, and L bands, and all celestial directions are observed hundreds of times at all accessible solar elongation angles (depending upon ecliptic latitude) in the range 64° to 124°. The instrument is designed to achieve a sensitivity for each field of view of $\nu I(\nu) = 10^{-13}$ W cm^{-2} sr^{-1} (1 s, 1 year). This level is well below most estimated CIB contributions. Extensive modeling of the foregrounds, just beginning, will be required to isolate and identify any extragalactic component.

The DIRBE instrument is an absolute radiometer, utilizing an off-axis folded Gregorian telescope with a 19-cm diameter primary mirror. The optical configuration is carefully designed for strong rejection of stray light from the Sun, Earth limb, Moon or other off-axis celestial radiation, or parts of *COBE*. Stray light rejection features include both a secondary field stop and a Lyot stop, super-polished primary and secondary mirrors, a reflective forebaffle, extensive internal baffling, and a complete light-tight enclosure of the instrument within the *COBE* dewar. Additional protection is provided by the Sun and Earth shade surrounding the *COBE* dewar, which prevents direct illumination of the dewar aperture by these strong local sources. The DIRBE instrument, which is maintained at a temperature below 2 K within the dewar, measures absolute brightness by chopping between the sky signal and a zero-flux internal reference at 32 Hz using a tuning fork chopper. Instrumental offsets are measured by closing a cold shutter located at the prime focus. All spectral bands view the same instantaneous field-of-view, 0.7° x 0.7°, oriented at 30° from the spacecraft spin axis. This allows the DIRBE to modulate solar elongation angles by 60° during each rotation, and to sample fully 50% of the celestial sphere each day. Four highly-reproducible internal radiative reference sources can be used to stimulate all detectors when the shutter is closed to monitor the stability and linearity of the instrument response. The highly redundant sky sampling and frequent response checks provide precise photometric closure over the sky for the duration of the mission. Calibration of the photometric scale is obtained from observations of isolated bright celestial sources. Careful measurements of the beam shape in pre-flight system testing and during the mission using scans across bright point sources allow conversion of point-source calibrations to surface brightness calibrations.

Qualitatively, the initial DIRBE sky maps show the expected character of the infrared sky. For example, at 1.2 microns stellar emission from the galactic plane and from isolated high latitude stars is prominent. Zodiacal scattered light from interplanetary dust is also prominent. At fixed ecliptic latitude the zodiacal light decreases strongly with increasing solar elongation angle, and at fixed elongation angle it decreases with increasing ecliptic latitude. These two components continue to dominate out to 3.4 microns, though both become fainter as wavelength increases. The foreground emissions have relative minima at wavelengths of 3.4 microns and longward of 100 microns. A composite of the 1.2, 2.3, and 3.4 microns images is shown in Figure 1a. Because extinction at these wavelengths is far less than in visible light, the disk and bulge stellar populations of the Milky Way are dramatically apparent in this image. A composite of the 25, 60, and 100 micron images is shown in Figure 1b. At 12 and 25 microns, emission from the interplanetary dust dominates the sky brightness, again strongly dependent upon ecliptic latitude and elongation angle. At wavelengths of 60 microns and longer, emission from the interstellar medium dominates the galactic brightness, and the interplanetary dust emission becomes progressively less apparent. The patchy infrared cirrus noted in *IRAS* data is evident at all of these wavelengths. The DIRBE data will clearly be a valuable new resource for studies of the interplanetary medium and Galaxy as well as the search for the CIB.

IRAS measurements toward the south ecliptic pole have been compared with DIRBE results. The two experiments are seen to agree reasonably well at 12 and 25 microns, but the DIRBE results are substantially fainter at 60 and 100 microns, reaching a factor of 2.6 at 100 microns. We have made a more detailed comparison with *IRAS* data at several points on the sky. By choosing points of different brightness, we can distinguish zero-point offsets and gain differences. We find evidence for zero-point differences, evidently not constant in time, of a few MJy/sr at all *IRAS* wavelengths. These are most significant (as a fraction of total brightness) at the longest wavelengths. We also find that the *IRAS* dc gain at 60 and 100 microns is substantially too high, a result which can be understood in terms of the detector characteristics and the data reduction procedures used for *IRAS* image-format data (see the *IRAS* Explanatory Supplement (1988), pp. IV-9 and IV-10 for a discussion of the *IRAS* dc response). The combined effect of these discrepancies is particularly large at 100 microns toward faint sky regions. Since *IRAS* detector gain depends on source angular scale (a scan-modulated instrument) and source brightness, no simple conversion between the total brightness data from the two experiments is universally applicable. This discussion applies only to surface brightness measurements; point source flux calibration is not subject to similar problems.

The DIRBE flux limits (Hauser *et al.* 1991)[1] have the expected spectral shape. They can be compared in detail with other measurements, e.g. *IRAS*, ZIP, Matsumoto *et al.*, (1988A&B) and Noda *et al.* (1991). *IRAS* measurements toward the south ecliptic pole have been compared with DIRBE results. The two experiments are seen to agree reasonably well at 12 and 25 microns, but the DIRBE results are substantially fainter at 60 and 100 microns, reaching a factor of ~3 at 100 microns. The DIRBE and ZIP (Murdock & Price 1985) results at the north ecliptic pole agree to 10% at 10 and 20 microns. Comparison with Matsumoto *et al.* and Noda *et al.* shows fairly good agreement in the near infrared with a deeper minimum at 3.4 microns and reasonable agreement in the far infrared but not as sharp a bump at 160 microns. These results and interpretations are discussed in the lecture by Bernard Carr and, for example, a paper by Bond, Carr, & Hogan (1991). The DIRBE (and FIRAS) data already rule out significant early VMO's and explosions and constrain galactic evolution models. The DIRBE data will clearly be a valuable new resource for studies of the interplanetary medium and Galaxy as well as the search for the CIB.

The DIRBE team is headed by the Principal Investigator Micheal Hauser and Deputy Principal Investigator Tom Kelsall. In addition to the *COBE* SWG participation the following people are working on DIRBE: S. Burdick, G. N. Toller, G. Berriman, B. B. Franz, K. J. Mitchell, M. Mitra, N. P. Odegard, F. S. Patt, W. J. Speisman, S.W. Stemwedel, J. A. Skard, A. Ahearn, W. Daffer, I. Freedman, S. Jong, A. Panitz, A. Ramsey, T. Roegner, V. Snowel, K. Tewari, H. T. Freudenreich, C. Lisse, J. Weiland.

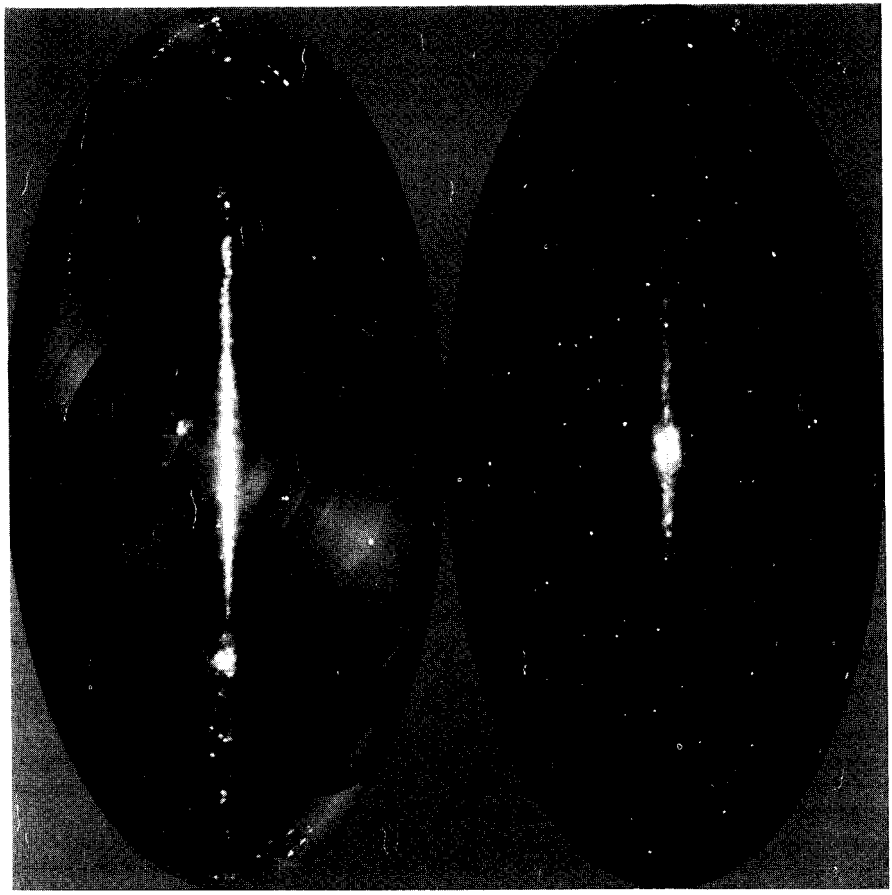

Figure 1. *COBE* DIRBE full sky maps in galactic coordinates. 1A. Combined 1.2, 2.2, and 3.4 micron map in respective blue, green, and red colors. The image shows both the thin disk and central bulge of the galaxy. 1B. Combined 25, 60, and 100 micron map in respective blue, green, and red colors. Both maps are preliminary results of a full sky scan by the DIRBE instrument. The discontinuities apparent are due primarily to the change in zodiacal light as the spacecraft and earth move around in the zodiacal dust but may in part be due to not having final instrument calibration.

3. FIRAS Instrument Description and CMB Spectrum Results

The FIRAS compares the spectrum of the CMB with that of a precise blackbody, enabling the measurement of very small deviations from a Planckian spectrum. The FIRAS instrument covers two frequency ranges, a low frequency channel from 1 to 20 cm^{-1} and a high frequency channel from 20 to 100 cm^{-1}. It has a 7° diameter beam width, established by a non-imaging parabolic concentrator, which has a flared aperture to reduce diffractive sidelobe responses. The instrument is calibrated by a full beam, temperature-controlled external blackbody, which can be moved into the beam on command. The FIRAS is the first instrument to measure the background radiation and compare it with such an accurate external full-beam calibrator in flight. The spectral resolution is obtained with a polarizing Michelson interferometer, with separated input and output beams to permit fully symmetrical differential operation. One input beam views the sky or the full aperture calibrator, while the second input beam views an internal temperature controlled reference blackbody, with its own parabolic concentrator. Both input concentrators and both calibrators are temperature controlled and can be set by command to any temperature between 2 and 25 K. In standard operating condition the two concentrators and the internal reference body are commanded to match the sky temperature, thereby yielding a nearly nulled interferogram and reducing almost all instrumental gain errors to negligible values.

The external calibrator determines the accuracy of the instrument for broad band sources like the CMBR. It is a re-entrant cone shaped like a trumpet mute, made of Eccosorb CR-110 iron-loaded epoxy. The angles at the point and groove are 25°, so that a ray reaching the detector has undergone 7 specular reflections from the calibrator. The calculated reflectance for this design, including diffraction and surface imperfections, is less than 10^{-4} from 2 to 20 cm^{-1}. Measurements of the reflectance of an identical calibrator in an identical antenna using coherent radiation at 1 cm^{-1} and 3 cm^{-1} frequencies confirm this calculation. The instrument is calibrated by measuring spectra with the calibrator in the sky horn while operating all other controllable sources within the instrument at a sequence of different temperatures.

The first results of the FIRAS[2] may be summarized as follows: The intensity of the background sky radiation is consistent with a blackbody at 2.735 ± 0.06 K. Deviations from this blackbody at the spectral resolution of the instrument are less than 1% of the peak brightness. The quoted error is primarily due to an uncertainty in the thermometer calibration; we expect to reduce this uncertainty by additional tests. The measured spectrum is shown in Figure 2, and is converted to temperature units, where it is compared to previous measurements. The deviations can be fitted to the Sunyaev-Zel'dovich form for Comptonization[3], giving a limit of $|y| < 10^{-3}$ (3σ). A fit to a Bose-Einstein distribution gives a limit on the dimensionless chemical potential of $|\mu| < 10^{-2}$ (3σ). This places a strong limit on the existence of a smooth hot intergalactic medium: it can contribute less than 3% of the X-ray background radiation even at a reheating time as recent as z=2. There is no evidence of a spectral distortion, such as that reported by Matsumoto *et al.*[4], and the measured temperature is consistent with previous reports and the recent rocket result of Gush *et al.*[5].

The variation of the spectrum with sky position as measured by the FIRAS is dominated by the dipole anisotropy of the CMB, plus a variation in the interstellar dust emission. A preliminary dipole anisotropy spectrum was determined by calculating the average spectra in two large circular regions of the sky each of angular diameter 60°, one centered at (α, δ) = (11.1h, -6.3°) and the other at (23.1h, 6.3°), which lie along opposite ends of the dipole axis as determined by the DMR. The difference between these spectra is fit extremely well by the difference of two blackbodies, and is consistent with a peak dipole amplitude of 3.3 ± 0.3 mK and the assumed dipole direction.

These precise limits to potential distortions covering the major portion of the CMB photons provide support for a key element in the models of Big Bang nucleosynthesis - the baryon to photon ratio and the interpretation of that number relative to the critical density. The FIRAS measurement actually counts the vast majority of photons and the precision of the measurement gives us the density constraint

$$\rho_\gamma = 4.722\ (T/1K)^4 e^{4y}\ eV/cm^3 \sim 10^{-33}\ (To/2.7K)^4 e^{4y}\ gm/cm^3$$

$$n_\gamma = 20.286\ (T/1K)^3\ \text{photons/cm}^3 = 415\ (To/2.735K)^3\ \text{photons/cm}^3 \qquad (1)$$

The FIRAS measurements decrease the error on n_g from greater than 20% to less than 5%. The limits on |μ| and |y| in tum limit energy release in the early universe ($1+z < few\ 10^6$) to typically less than 1% of the energy in the CMB. This in tum provides limit on cosmologically significant events such as primordial particle decay, superconducting cosmic strings, and turbulence. A currently interesting restriction is on the parameters of neutrinoes that decay to photons. Examples at hand are a potential 17 keV neutrino and Sciama's 28 eV neutrino. The 17 keV neutrino lifetime cannot be between 1 year and about 10^{12} years because it would either distort the CMB spectrum or its decay photons must show up directly. Sciama's proposed 28 eV neutrino is similarly restricted but Sciama has cleverly proposed a sufficiently long lifetime and hidden the decay photons in the ultravoliet background.

The FIRAS instrument also measures the galactic emission and has made a survey of the dust and line emission in its bands. The dust emission is strong; the FIRAS provides good spectral information on that dust and has found some ten emission lines (Wright *et al.* 1991). In addition FIRAS has produced maps of the dust emission (205 μm for instance), the 205 μm NII line and 158 μm CII line.

The FIRAS team is headed by the Principal Investigator John Mather, Deputy Principal Investigator Rick Shafer and Deputy Project Scientist for Data Ed Cheng. In addition to the *COBE* SWG participation the following people are working on FIRAS: Dale Fixsen, Gene Eplee, Joel Gales, Rich Isaacman, Snehevadan Macwan, Derck Massa, Muriel Taylor, Alice Trenholme, Dave Wynne, Steve Alexander, Dave Bouler, Nilo Gonzalez, Ken Jensen, Shirley Read, Larry Rosen, Fred Shuman, Frank Varosi, Harte Wang, Will Daffer, Jim Krise, Nick Iascone, and Courtney Scott.

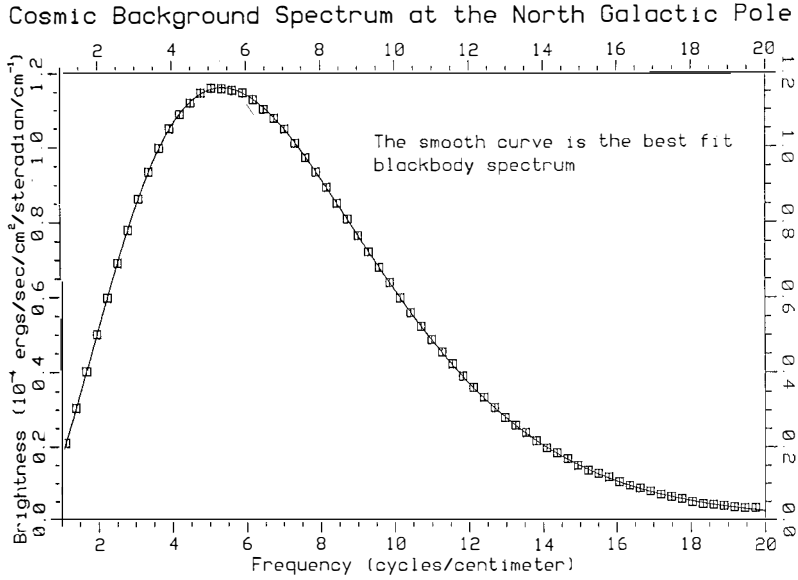

Figure 2. ***COBE*** **FIRAS spectrum measurement. The boxes are the data points and the line the best fit Planckian (2.735 K). The data are taken near the north galactic pole.**

4. DMR

4.1 DMR Instrument Description and Operation

The *COBE* Differential Microwave Radiometers (DMR) instrument is intended to provide precise maps of the microwave sky on large angular scales. It consists of six differential microwave radiometers, two independent radiometers at each of three frequencies: 31.5, 53, and 90 GHz (wavelengths 9.5, 5.7, and 3.3 mm). At these frequencies the CMB dominates foreground galactic emission by at least a factor of roughly 1000. The multiple frequencies allow subtraction of galactic emission using its spectral signature, yielding maps of the CMB and thus the distribution of matter and energy in the early universe. Each radiometer measures the difference in microwave power between two regions of the sky separated by 60°. The combined motions of spacecraft spin (75 s period), orbit (103 minute period), and orbital precession (~1 degree per day) allow each sky position to be compared to all others through a massively redundant set of all possible difference measurements spaced 60° apart.

Each radiometer consists of a superheterodyne receiver switched at 100 Hz between two identical corrugated-horn antennas. The compact low-sidelobe antennas' main beam profile is well described by a Gaussian of 7° FWHM and point 60° apart, 30° to either side of the spacecraft spin axis[6]. The two channels at 31.5 GHz share a single antenna pair with an orthomode transducer splitting the input into opposite circular polarizations. Both channels share a common enclosure and thermal regulation system. The 53 and 90 GHz radiometers are similar but have two antenna pairs at each frequency, each with identical linear polarization response. A detailed description of the DMR instrument may be found in Smoot *et al.*[7].

Three independent techniques are used to determine the radiometer calibration. Solid-state noise sources provide in-flight calibration by injecting broad-band microwave power into the front end of each radiometer at regular intervals (every two hours). Prior to launch the noise source signals were calibrated by comparing to the signal produced by targets of known, dissimilar temperatures (approximately 300 K and 77 K) covering the antenna apertures. The DMR observes the Moon for a fraction of an orbit during two weeks of every month providing an independent determination of the calibration factor. The Earth's ~30 km s^{-1} motion about the solar system barycenter produces a Doppler-shift dipole of known magnitude (~0.3 mK) and direction. The modulation in amplitude and direction is apparent, but at low signal to noise. Given sufficient observing time (> one year), this method may produce the most accurate determination of the absolute calibration of the DMR instrument. A forthcoming paper[8] discusses the DMR calibration more fully.

The DMR has been operating well since about a week after the *COBE* launch (18 Nov 1989) and is approved for two years of operation. Two additional years of operation have been requested.

4.2 DMR Data Reduction and Analysis

A software analysis system receives data telemetered from the satellite, determines the instrument calibration, and inverts the difference measurements to map the microwave sky in each channel. Although the experiment has been designed to minimize or avoid sources of systematic uncertainty, both the instrument and the software can potentially introduce systematic effects correlated with antenna pointing, which would create or mask features in the final sky maps. Further details of the data processing algorithms may be found in Torres *et al.* [9]

The sky maps may in principle contain contamination from local sources or artifacts from the data reduction process itself. The data reduction process must distinguish cosmological signals from a variety of potential systematic effects. The most obvious source of non-cosmological signals is the presence in the sky of foreground microwave sources. These include thermal emission from the *COBE* spacecraft itself, from the Earth, Moon, and Sun, and from other celestial objects. Non-thermal radio-frequency interference (RFI) must also be considered, both from ground stations and from geosynchronous satellites. Although the DMR instrument is largely shielded from such sources, their residual or intermittent effect must be considered. A second class of potential systematics is the effect of the changing orbital environment on the instrument. Various instrument components have slightly different performance with changes in temperature, voltage, and local magnetic field, each of which can be modulated by the *COBE* orbit. Longer-term drifts can also affect the data. Finally, the data reduction process itself may introduce or mask features in

the data. The DMR data are differential; the sparse matrix algorithm is subject to concerns of both coverage (closure) and solution stability. Other features of the data reduction process, particularly the calibration and baseline subtraction, are also a source of potential artifacts. All potential sources of systematic error must be identified and their effects measured or limited before maps with reliable uncertainties can be produced.

The largest limit is the current 5% uncertainty in the absolute calibration of the instrument. The uncertainty in absolute calibration does not create artifacts in the maps but affects the calculated amplitude of existing features (e.g., the dipole anisotropy). We continue to acquire and analyze calibration information and we anticipate improved calibration in the future. The next largest effect is the modulation of the instrument output in the Earth's magnetic field; the primary effect is on the dipole term of a spherical harmonics expansion. The magnetic effects will be modelled and removed in future analysis. The 53A channel unambiguously shows a magnetic susceptibility; we do not include the 53A channel in the dipole results presented below. The largest potential effects upon the quadrupole and higher-order multipole coefficients are Earth emission and the possibility of undetected calibration drifts. The current 95% C.L. upper limits to combined systematic errors in the DMR maps are $\Delta T/T_0 < 8x10^{-5}$ for the dipole anisotropy and $\Delta T/T_0 < 3x10^{-5}$ for the quadrupole and higher-order terms.

As the DMR gathers redundant sky coverage and as analysis continues, we anticipate refined estimates of, or limits on, these effects. It is important to note, however, that the DMR is free from some of the systematics of previous large-scale sky surveys. The multiple differences generated by various chopping frequencies (spin, orbit, and precession periods) allow separation of instrumental from celestial signals. Two independent full-sky maps, produced with matched beams at each of three frequencies, provide a powerful tool for analysis and removal of possible systematic effects.

4.3 DMR RESULTS

Figure 3 shows the microwave sky at 6 mm on a linear scale. The most noticeable effect is the extreme uniformity of the CMB. The preliminary maps of the microwave sky for each of the six DMR channels look very nearly the same in terms of the dipole while the galactic emission varies with frequency. The independent maps at each frequency enable celestial signals to be distinguished from noise or spurious features: a celestial source will appear at identical amplitude in both maps. The three frequencies allow separation of cosmological signals from galactic foregrounds based on spectral signatures. The maps are corrected to solar-system barycenter and do not include data with the Moon within 25° of an antenna; no other systematic corrections have been made. All six maps clearly show the dipole anisotropy and galactic emission. The dipole appears at similar amplitudes in all maps while galactic emission decreases sharply at higher frequencies, in accord with the expected spectral behavior.

An observer moving with velocity $\beta = v/c$ relative to an isotropic radiation field of temperature T_0 observes a Doppler-shifted temperature

$$T = T_0 \frac{(1 - \beta^2)^{1/2}}{1 - \beta\cos(\theta)} = T_0 [\, 1 + \beta\cos(\theta) + \frac{1}{2}\beta^2 \cos(2\theta) + O(\beta^3) \,] \qquad (2)$$

The first term is the monopole CMB temperature without a Doppler shift. The second term, proportional to b, is a dipole distribution, varying as the cosine of the angle between the velocity and the direction of observation. The term proportional to b^2 is a quadrupole with amplitude reduced by 1/2 b from the dipole amplitude. The DMR maps clearly show a dipole distribution consistent with a Doppler-shifted thermal spectrum, implying a velocity for the solar system barycenter of $\beta=0.00123 \pm 0.00003$ (68% CL), or $v = 370\pm10$ km s^{-1} toward $(l, b) = (264°\pm2, 49°\pm2°)$, where we assume a value $T_0=2.735$ K. The solar system velocity with respect to the local standard of rest is estimated at 20 km s^{-1} toward (57°,23°), while galactic rotation moves the the local standard of rest at 220 km s^{-1} toward (90°,0°)[10,11]. The DMR results thus imply a peculiar velocity for the Galaxy of $v_g = 550 \pm 10$ km s^{-1} in the direction (266° ± 2°, 30° ± 2°). This is in rough agreement with independent determinations of the velocity of the local group, $v_{lg} = 507 \pm 10$ km s^{-1} toward (264 °± 2°, 31° ± 2°)[12].

The angular distribution on the full sky maps is fully consistent with a dipole anisotropy. The spectrum of all published dipole parameters, including those from the *COBE* FIRAS experiment[2], is consistent with a Doppler-shifted blackbody origin. With high probability the dipole comes from peculiar motion and is not due to an intrinsic dipole either large scale gradient as suggested by Paczynski and Piran (1990) or net velocity of CMB relative to comoving frame[13]. The CMB dipole anisotropy is well established by the chi-squared of the dipole fit and the dipole amplitude spectrum. The dipole anisotropy is more than 30 times larger than any other large angular scale anisotropy. The dipole anisotropy is then either due to a Doppler shift or is intrinsic temperature anisotropy. It is very difficult to establish a universe with a large dipole anisotropy without comparable quadrupolar and higher order moment anisotropies We can compare the dipole anisotropy implied velocity with the velocity expected due to gravitational perturbations in the region 100 Mpc around our location. Our peculiar velocity can be estimated either by adding up observed sources (light⇒mass⇒potential), e.g. *IRAS* galaxies or by inferring potential from observing large scale velocity flows, e.g. the "Great Attractor", that one readily obtains 80% of the CMB dipole implied velocity. The errors in this calculation are on the order of 20% or greater so that the whole dipole anisotropy can easily be explained as due to the peculiar velocity of our galaxy. Thus we adopt the working hypothesis that the dipole is generated by the galactic peculiar velocity to the comoving frame and the resulting Doppler shift.

The DMR maps with this dipole removed from the data show the only large-scale feature remaining is galactic emission, primarily confined to the plane of the galaxy. This emission is present at roughly the level expected before flight and is consistent with emission from electrons (synchrotron and HII) and dust within the galaxy. The ratio of the dipole anisotropy (the largest cosmological feature in the maps) to the Galactic foreground reaches a maximum in the frequency range 60—90 GHz. There is no evidence of any other emission features.

We have made a series of spherical harmonic fits to the data, excluding data within several ranges of galactic latitude. The only large-scale anisotropy detected to date is the dipole. The quadrupole anisotropy is limited $\Delta T/T < 3 \times 10^{-5}$ and higher-order terms are limited to amplitude $\Delta T/T < 10^{-4}$. Similarly, a search for Gaussian or non-Gaussian fluctuations on the sky showed no features to limit $\Delta T/T < 10^{-4}$. The results are insensitive to the precise cut in galactic latitude and are consistent with the expected Gaussian instrument noise. The reported uncertainties are 95% confidence level unless otherwise stated, and include the effects of systematics as listed in Table 1.

These limits on the quadrupole are somewhat better than previous anisotropy studies, but are still limited by uncertainties in estimates of many systematic errors that may well be removed in further data processing. In an ideal case this might result in a 95% confidence level upper limit of < 5μK on the rms quadrupole. One important systematic error term that may well ultimately limit the detectable quadrupole and other large angular scale anisotropies is galactic emission. The rms quadrupole amplitude including galactic emission (DMR 31, 53, and 90 GHz data and the Relict 37 GHz data) decreases with increasing frequency. However, since the CMB amplitude begins to decrease with frequency, the DMR 53 and 90 GHz channels bracket the apparent best observing frequency range. Including the galactic plane produces a quadrupole amplitude at minimum of 50 μK. To obtain ultimate sensitivity we need a level 20 to 30 times lower. How much does simply cutting the galactic plane from the fitting achieve? Tests using the 408 MHz and *IRAS* 100 micron maps indicate that reasonable galactic latitude cuts gain roughly a factor of 5 to 10. We will have to obtain the remaining factor of 2 to 4 from careful modeling.

4.4 DMR DISCUSSION

The DMR limits to CMB anisotropies provide significant new limits to the dynamics and physical processes in the early universe. The dipole anisotropy provides a precise measure of the Earth's peculiar velocity with respect to the co-moving frame. Limits to higher-order anisotropies limit global shear and vorticity in the early universe. If the universe were rotating (in violation of Mach's Principle), the resultant metric causes null geodesics to spiral; in a flat universe the resultant anisotropy is dominated by a quadrupole term[13,14]. The limit $\Delta T/T < 3 \times 10^{-5}$ for quadrupole and higher spherical harmonics limits the rotation rate of universe to $\Omega < 3 \times 10^{-24}$ s^{-1}, or less than one ten-thousandth of a turn in the last ten billion years.

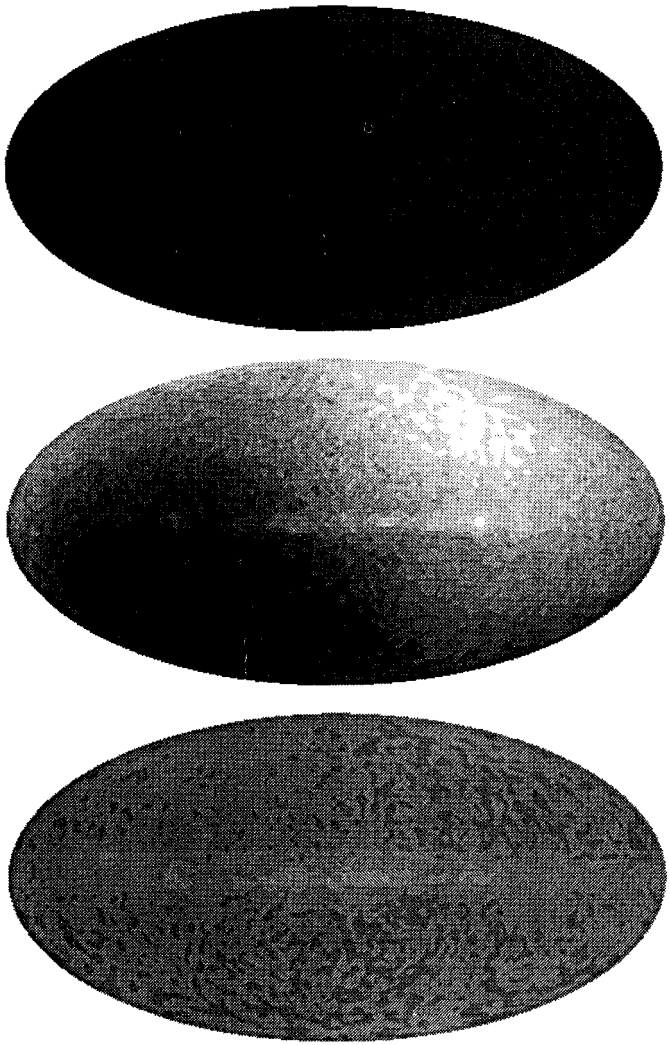

Figure 3 *COBE* DMR full sky maps of the temperature of the sky at 53 GHz (6 mm wavelength). The maps are in galactic coordinates and have been corrected to solar system barycenter.

3.A Absolute Sky Brightness on a scale from 0 to 3.6 K

3.B Relative sky brightness with mean removed and scale to about -4 to +4 mK. The dipole anisotropy (0.1%) and galactic plane are clearly visible.

3.C Relative sky brightness with monopole and dipole removed. The galactic plane is only significant visible signal. The other structure evident is consistent with instrument observing noise.

If the expansion of the universe were not uniform, the expansion anisotropy would lead to a temperature anisotropy in the CMB of similar magnitude. The large-scale isotropy of the DMR results indicate that the Hubble expansion is uniform to one part in 10^4. This provides additional evidence for hot big bang models of cosmology, and indicates that the currently observed expansion of the universe can be traced back at least to the radiation-dominated era.

Inhomogeneities in the density in the early universe also lead to temperature anisotropies in the CMB as the CMB photons climb out of varying gravitational potential wells[15,16]

$$\Delta T/T \approx \frac{1}{2}\left(\frac{\delta\rho}{\rho}\right)_L \left(\frac{H_o L}{c}\right)^2 = \frac{1}{2}\left[\frac{L}{L_o}\right]^2 \left(\frac{\delta\rho}{\rho}\right)_L \qquad (3a)$$

The DMR results imply that the universe at the surface of last scattering was isotropic and homogeneous to the 10^{-4} level.

Inhomogeneities on scales outside the present horizon induce gradients and shear across the region within our horizon, and these cause anisotropy in the CMB. Grischuk and Zel'dovich[16] (1978) have shown that a very long wavelength density ripple in a spatially flat universe generates a quadrupole anisotropy in the CMB.

$$\left(\frac{\Delta T}{T}\right)_{quadrupole} \approx L_o^2 \nabla^2\delta\phi = (c/H_o)^2 \nabla^2\delta\phi \approx \frac{1}{2}\left[\frac{L_o}{L}\right]^2 \left(\frac{\delta\rho}{\rho}\right)_L \qquad (3b)$$

There is no dipole term because both the photons and the observer are in free fall. The effect that matters is the potential gradient associated with the inhomogeneities. If the universe is flat, the DMR limits on the quadrupole term constrain $(\delta\rho/\rho)_L < 10^{-4}\,(L/L_o)^2$. Inspite of what one might have thought, we can tell something about structure outside our present horizon up to of order 100 times the present horizon. The large scale geometry of the universe is thus well-described by a Robertson-Walker metric with only local perturbations.

One such potential local perturbation is gravitational radiation. Long-wavelength gravitational waves propagating though this region of the universe distort the metric and produce a quadrupole distortion in the CMB[17]. The limits $\Delta T/T < 3 \times 10^{-5}$ for quadrupole restricts the energy density of single plane waves or a chaotic superposition to

$$\Omega_{gw} < 3 \times 10^{-4} \left(\frac{\lambda_{gw}}{10\ Mpc}\right)^{-2} h^{-2} \qquad (4a)$$

where Ω_{gw} is the energy density of the gravity waves relative to the critical density, λ_{gw} is the wavelength at the current epoch, and h is the Hubble constant in units 100 km s^{-1} Mpc^{-1}.

Those gravity waves on the surface of last scattering will produce chaotic fluctuations. The DMR is sensitive primarily to gravitational waves with scale sizes > 7° at the surface of last scattering, or ~200 Mpc today. The temperature anisotropy observed is roughly half the strain that a freely falling observer at the surface of last scattering would observe. To determine the presnt energy density of the gravity waves present at the surface of last scattering one must propagate the waves to the present. A number of factors compensate and the limit is essentially independent of wavelength and is about

$$\Omega_{gw\text{-}lss} < 1/3 \left[\frac{\Delta T}{T}\right]^2 \approx 3 \times 10^{-10} \qquad (4b)$$

Cosmic strings provide another mechanism for local distortions in the metric. They are nearly one-dimensional topological defects predicted by many particle physics gauge theories and are characterized by a large mass per unit length, μ[18]. The large mass and relativistic velocity produce CMB anisotropies through the relativistic boost and the Sachs-Wolfe effect (gravitational lensing alone does not produce anisotropy in an otherwise isotropic background). Many authors have calculated the anisotropy produced by various configurations of cosmic strings, with typical values[19,20]

$$\Delta T/T \sim 8\pi\beta\gamma\frac{G\mu}{c^2} \qquad (5)$$

The DMR experiment limits the existence of large-scale cosmic strings to $G\mu/c^2 < 10^{-5}$. There is no evidence for higher-order topological defects such as domain walls or textures. The large scale geometry of the universe appears to be uniform and without defects.

The observed isotropy of the universe on large angular scales presents a major problem for cosmology. At the time of primordial nucleosynthesis the presently observable universe was divided into about 10^{25} causally independent regions. The observed uniformity of light elements implies a baryon density uniformity of $\delta\rho/\rho < 3$ during synthesis[21]. At the surface of last scattering the horizon size subtends ~2° when viewed from here. Regions separated by more than 2° were not in causal contact; consequently, DMR measures some 10^4 causally disconnected regions of the sky. Standard models of cosmology fail to explain why causally unconnected regions are the same to order unity, much less the 10^{-4} isotropy implied by the DMR observations. Inflationary scenarios provide one solution. In these models, the universe undergoes a spontaneous phase transition ~10^{-32} seconds after the Big Bang, causing a period of exponential growth in which the scale size increases by 30 to 40 orders of magnitude. The entire observed universe would then originate from a small pre-inflationary volume in causal contact with itself, eliminating the problem. In the simplest inflationary models, the pre-inflationary matter and radiation fields are diluted to zero along with any pre-existing anisotropies. The process of inflation, however, generates scale-free anisotropies with a Harrison-Zel'dovich spectrum which result in small but detectable CMB anisotropies in the present universe[22,23]. During inflation zero point quantum fluctuations produce density fluctuations and gravitons (scalar and tensor fields) at levels comparable to the vacuum energy. Thus at the horizon wavelength scales they should produce comparable CMB anisotropies. The CMB anisotropy limits are now just pushing down to the level which is needed for observed velocities/gravitational potentials and begining to limit the energy scale of inflation at a natural level. If we were optimistic, we could hope to see anisotropies at the 10^{-5} level, giving us the density fluctuations we need and telling us the inflation energy scale.

Inflationary models predict quadrupole temperature fluctuations from gravitons or density fluctuations of order $\Delta T/T \sim H / M_{Planck}$, where H is the Hubble parameter during inflation (a period characterized by a constant Hubble parameter). As a result, the possible values of the Hubble parameter at the inflationary stage are significantly restricted by the anisotropy limits.

The relationship between the inflation vacuum Hubble parameter and the vacuum energy density is

$$H^2 = 8\pi/3\ G\ \rho_{vacuum} = 8\pi/3\ G\ M^4 = 8\pi/3\ M^4 / M_{Planck}^2 \quad (6)$$

where M is the energy scale of inflation and energy density of the vacuum, $\rho_{vacuum} = M^4$. The energy density of gravitons (see Figure 4) is

$$\Omega_{graviton} = 10^{-4}\ \rho_{vacuum}/ M_{Planck}^4 = 10^{-4}\ (M/M_{Planck})^4 \quad (7)$$

for wavelengths significantly smaller than the horizon, rising to $\rho_{vacuum}/ M_{Planck}^4 = (M/ M_{Planck})^4$ at horizon size. The quadrupole CMB anisotropy and smaller angular scales limits imply $H_{inflation} < 3\ 10^{-5}\ M_{Planck}$, the inflation energy scale is far removed from the Planck scale ($M < 10^{17}$ GeV), and the energy density of the vacuum is $\rho_{vacuum} = M^4 < 10^{-9}\ M_{Planck}$. There is thus some reason to expect that the phase transition for grand unification (GUT) and the phase transition producing inflation are intimately related. The measurements are forcing the energy scale of each into the same region. After being separated for theoretical freedom and generalness, experiments may reunite them as in the original motivation. There would be a certain economy and beauty in having inflation and grand unification occur through the same mechanism and it would join together particle physics and cosmology at the birth of the universe.

A second major problem in cosmology is the growth of structure in the universe. The largest structures in the current universe (walls and voids) are observed to have density fluctuations $\delta\rho/\rho$ of order unity on scale sizes ~50 Mpc. Structures of this size are at the horizon scale at the surface of last scattering; consequently, the primordial density fluctuations are small and most of the

growth is in the linear regime. The assumption of linear growth requires peculiar velocities ~ 0.01c in order to move the matter the required 10^8 light years of co-moving distance in the ~10^{10} years estimated to have elapsed since the surface of last scattering, an order of magnitude greater than the peculiar velocity inferred from dipole anisotropy. To explain the observed structure without violating limits on CMB anisotropy, and to generate the critical density required by inflationary models, many astrophysicists have turned to cosmological models in which most of the matter in the universe (> 90%) is composed of weakly interacting massive particles (WIMPs). The dynamical properties of this "dark matter" allow it to clump faster than the baryonic matter, which later falls into the WIMP gravitational potential wells to form the structures observed today. The gravitational potential and motion of these particles produce CMB anisotropy whose amplitude depends on the angular scale size. For scale size ~ 10° most reasonable models predict $\Delta T/T \sim 1$—3×10^{-5}, depending on the average density of the universe[24]. Although current observations do not provide significant limits to these models, we anticipate that the DMR will provide a stringent test of such models as it continues to accumulate data.

The DMR team is headed by the Principal Investigator George F. Smoot and Deputy Principal Investigator Charles Bennett. In addition to the *COBE* SWG participation the following people are working on DMR: Alan Kogut, Jon Aymon, Charles Backus, Giovanni De Amici, Kevin Galuk, Gary Hinshaw, Peter D. Jackson, Phil Keegstra, Robert Kummerer, Charles Lineweaver, Laurie Rokke, Luis Tenorio, Richard Mills, Jairo Santana, and Peter Young.

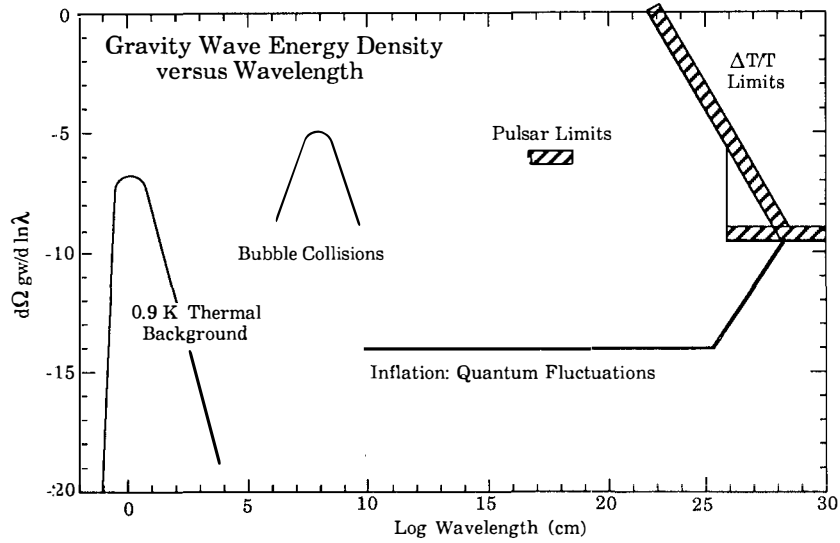

Figure 4. Limits on the energy density of long wavelength gravity waves. The DMR experiment sets two limits based upon the $\Delta T/T$ and strain to energy density relationships shown here and upon the formulas from Linder (1988): one is for the quadrupole and the other the surface of last scattering. The quantum fluctation curve is the predicted spectrum from inflation at maximum allowed normalization. This maximum curve corresponds to an energy scale of inflation slightly less than 10^{17} GeV. The potential inflation bubble collision spectrum is from Turner and Wilczek (1990). The normalization on the predictions depend upon the choice of elementary particle theory.

5. CONCLUSIONS

A year after launch, the *COBE* instruments are working well and continue to collect data. FIRAS has measured the CMB spectrum quite precisely and future improvements and maps are are expected. The FIRAS and DMR data show the expected dipole anisotropy, consistent with a Doppler-shifted thermal spectrum. Galactic emission is present at levels close to those expected prior to launch, and is largely confined to the plane of the galaxy. The results are currently limited by instrument noise and upper limits to potential sources of systematic error. There is no evidence for any other large-scale feature in the DMR maps. The DMR results limit CMB anisotropies on all angular scales >7° to $\Delta T/T < 10^{-4}$. The results are consistent with a universe described by a Robertson-Walker metric and show no evidence of anisotropic expansion, rotation, or defects (strings, walls, texture). As DMR sky coverage improves and the instrument noise per field of view decreases, we anticipate improved calibration, better estimates of potential systematics, and increasingly sensitive limits to potential CMB anisotropies. In principle, the DMR is capable of testing predictions of both inflationary and dark-matter cosmological models. DIRBE has produced exceptionally good and complete maps of the 1 to 300 micron sky.

ACKNOWLEDGEMENTS

The *COBE* instruments and satellite have been working well and continue to collect data due to the excellent work by the staff and management of the *COBE* Project. It is a pleasure to thank and acknowledge their work and great success. The COBE research is a team effort including some 19 original Science Working Group members and other scientists (see for example, Smoot *et al.*). This work supported in part by the Director, Office of Energy Research, Office of High Energy and Nuclear Physics, Division of High Energy Physics of the U.S. Department of Energy under Contract No. DE-AC03-76SF00098. We express our appreciation of Tran Thanh van and the Moriond group for organizing this meeting.

6. REFERENCES

1. Hauser, M. G. *et al.* 1991, "After the First Three Minutes", AIP, Holt, Bennett, & Trimble
1a. Matsumoto, T., Akiba, M., & Murakami, H, 1988A, *Ap. J.*, **332**, 575.
1b. Murdock, T. L., & Price, S. D. 1985, *Astr. J.*, **90**, 375.
1c. Noda *et al.* (1991) preprint
2. Mather *et al.* 1990a, *Ap. J.*, **354**, L37-L41.,Cheng *et al.* 1990, *Bull. APS*, **35**, 937.
3. Zel'dovich Ya. B. and Sunyaev R. A. 1969, *Ap. Space Sciences*, **4**, 301.
4. Matsumoto *et al.* (1988B), *Ap. J.*, **329**, 567-571.
5. Gush, H.P., Halpern, M. & Wishnow, E. (1990) *Phys. Rev. Lett.*, **35**, 937.
6. Toral, M.A., *et al.*, *IEEE Transactions on Antennas and Propagation*, **37**, 171 (1989).
7. Smoot, G.F., *et al.*, *Ap. J.*, **360**, 685 (1990). also *Ap. J. Let.*, **371**,L1.
8. Bennett, C.L., *et al.*, in preparation.
9. Torres, S., *et al.*, *Data Analysis in Astronomy*, ed. Di Gesu *et al.*, Plenum Press (1990).
10. Kerr, F.J., and Lyndon-Bell, D., *MNRAS*, **221**, 1023 (1990).
11. Fich, M., Blitz, L., and Stark, A., *Ap. J.*, **342**, 272 (1989).
12. Yahil, A., Tamman, A., and Sandage, A., *Ap. J.*, **217**, 903 (1977).
13. Collins, C.B., and Hawking, S.W., *MNRAS*, **162**, 307 (1973).
14. Barrow, J.D., Juskiewicz, R., and Sonoda, D.H., *MNRAS*, **213**, 917 (1985).
15. Sachs, R.K., and Wolfe, A.M., *Ap. J.*, **147**, 73 (1967).
16. Grischuk, L.P., and Zel'dovich, Ya. B., *Sov. Astron.*, **22**, 125 (1978).
17. Burke, W.L., *Ap. J.*, **196**, 329 (1975).
18. Vilenkin, A., *Physics Reports*, **121**, 263 (1985).
19. Stebbins, A., *Ap. J.*, **327**, 584 (1988).
20. Stebbins, A., *et al.*, *Ap. J.*, **322**, 1 (1987).
21. Yang, J., *et al.*, *Ap. J.*, **281**, 493 (1984).
22. Gorski, K., *Ap. J. Lett.* **370**, L5. (1991).
23. Abbott, L.F., and Wise, M.B., *Ap. J. Lett.*, **282**, L47 (1984).
24. Bond, J.R. and Efstathiou, G, *Ap. J. Lett.*, **285**, L45 (1984).